Bending Strength of Steel Bracket and Splice Plates

BENJAMIN A. MOHR and THOMAS M. MURRAY

Bracket plates typically support spandrel beams, or crane rails for industrial applications as shown in Figure 1. Often, these plates are bolted to the column flanges. A similar connection is the bolted web splice connection shown in Figure 2, which is typically used in cantilever construction to control the location of inflection points and reduce the required moment strength of the beams. The primary purpose of this study was to determine the ultimate behavior of bracket and splice plates and to compare the results with various design models.

CURRENT DESIGN MODELS

The required flexural strength, M_r, for the bracket plate shown in Figure 1 is simply the required vertical load, P_r, times the distance from its point of application to the first column of bolts, e. Likewise, the commonly assumed required flexural strength of the web splice plate shown in Figure 2 is the required beam shear, V_r, times the distance from the centerline of the connection to the first column of bolts, e. The required flexural strength must be less than the design strength ϕM_n in LRFD and M_n/Ω in ASD, according to the AISC *Specification for Structural Steel Buildings* (AISC, 2005a), where M_n is the nominal flexural strength, ϕ is the LRFD resistance factor, and Ω is the ASD safety factor.

The 3rd Edition of the AISC *Manual of Steel Construction, Load and Resistance Factor Design* (AISC, 2001), gives two limit states: flexural yielding and flexural rupture, in the design example on pages 15–13. The nominal flexural strength for yielding is determined from

$$M_n = F_y S_{gross} \tag{1}$$

where F_y is the specified minimum yield stress, and S_{gross} is the gross elastic section modulus of the plate. The nominal flexural strength for rupture is given by

$$M_n = F_u S_{net} \tag{2}$$

where

F_u = specified minimum tensile strength
S_{net} = net elastic section modulus of the plate

However, no literature is cited to support these relationships, nor has any been found by the writers. Conceptually, the behavior assumed by Equation 2 should never occur, since S_{net} assumes an elastic stress distribution, whereas F_u only occurs after plastic behavior.

The 13th Edition of the AISC *Steel Construction Manual* (AISC, 2005b) also uses two limit states to check flexural strength. The nominal flexural yielding strength is determined from

$$M_n = F_y Z_{gross} \tag{3}$$

where

Z_{gross} = gross plastic section modulus

However, the design examples for bracket plates and coped beams use $F_y S_{gross}$ for this limit state (AISC, 2005c).

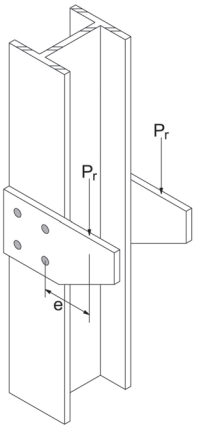

Fig. 1. Bracket plate connection.

Benjamin A. Mohr is a graduate assistant, Via Department of Civil and Environmental Engineering, Virginia Polytechnic Institute and State University, Blacksburg, VA.

Thomas M. Murray is Montague-Betts Professor of Structural Steel Design, Via Department of Civil and Environmental Engineering, Virginia Polytechnic Institute and State University, Blacksburg, VA.

The nominal flexural rupture strength is determined from

$$M_n = F_u Z_{net} \quad (4)$$

where

Z_{net} = net plastic section modulus

In an example for the design of a bolted beam web splice in *Analysis and Design of Connections* (Thornton and Kane, 1999), Equation 2 was used to determine the plate flexural rupture strength and Equation 3 was used for flexural yielding.

OVERVIEW OF STUDY

This study consisted of experimental testing and comparison of test results with various design methods. The experimental testing consisted of connecting two beams together with web splice plates to form a simple span, then loading the span symmetrically to induce pure moment at the location of the splice with the goal of achieving plate flexural rupture. The test setup is shown in Figure 3. The test results were compared to the predicted values from Equations 1 through 4, as well as a proposed design model.

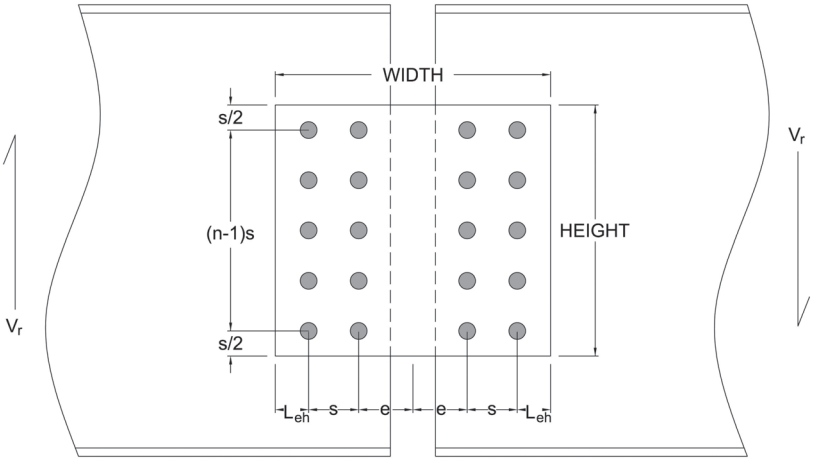

Fig. 2. Schematic representation of web splice plate.

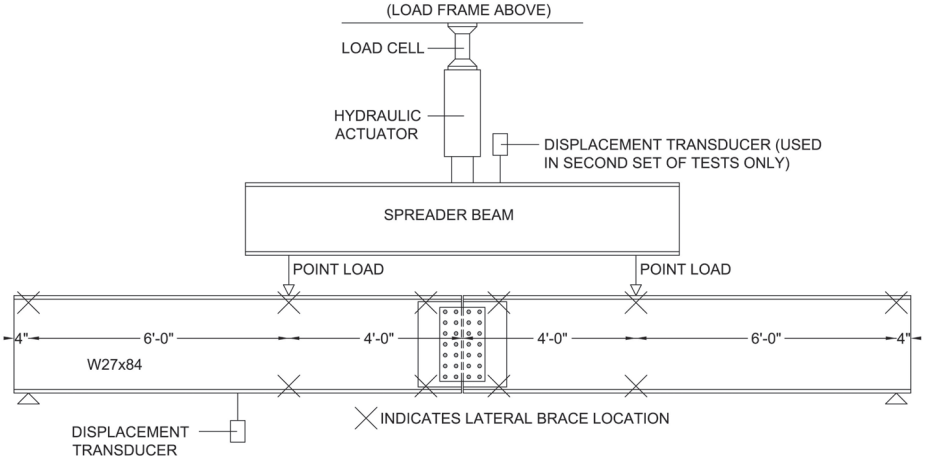

Fig. 3. Schematic diagram of test setup.

EXPERIMENTAL INVESTIGATION

Two series of splice plate tests were conducted. The first series consisted of six tests using three different bolt patterns with ⅜-in. plates and ¾-in.-diameter grade A490 bolts. The second series consisted of eight tests using both ⅜-in. and ⅝-in. plates and 1-in.-diameter grade A490 bolts. (Grade A490 bolts were used to eliminate the limit state of bolt shear.) For all tests, a plate was bolted to each side of the beam web.

The test setup (Figure 3) is not typical of standard construction. The large gap between the beams was required to accommodate the large deflections that occur prior to development of the plastic moment for the plates. If a smaller gap had been used, the top flanges of the beams would touch prior to plate rupture. Because of this large gap, the test setup experienced problems with stability, which are discussed below.

The test plates were checked for lateral-torsional buckling in accordance with the 2005 AISC Specification, Section F11.2 (AISC, 2005a). Using an unbraced length of 6.5 in. (the center-to-center distance between the innermost rows of bolts), lateral-torsional buckling was found not to be a controlling limit state for these tests.

Test Setup, Instrumentation and Procedures

The test setup consisted of two W27×84, A992 steel, beams, spliced together to form a simply supported 20-ft. span as shown in Figure 3. Two-point loading was used to create pure moment at midspan, and the connections were designed to ensure that the governing limit state would be flexural rupture of the plates.

The connection bolts were tightened with an impact wrench, except for two tests, where the bolts were snug-tightened using a spud wrench. No bolts were fully tightened.

Ten lateral braces were used, at the locations shown in Figure 3. Despite the braces, some out-of-plane movement of the beam compression flanges was observed at midspan during initial testing. To eliminate this movement, a channel, which fit tightly over the top flanges of both beams, was used to prevent the beams from rotating relative to each other. Also, during initial testing, lateral movement of the connection plates occurred. After some trial and error, an additional hole was punched at the centerline of the plate in line with the top row of bolts as shown in Figure 4. A bolt was passed through this hole, with washers inserted between the plates. The washers effectively prevented the plates from moving inward, and a snug-tight nut on the end of the bolt prevented outward movement.

Vertical deflections were measured for all tests using displacement transducers at the locations shown in Figure 3.

Test Specimens

Figure 4 shows the layout and dimensions for the splice plates. Each plate had either 3, 5 or 7 bolt rows, with all bolts spaced 3 in. on center. All vertical edge distances were 1½ in., and all horizontal edge distances were 2 in. The beam webs were punched for the seven row tests, and all plates were aligned with the beam centerline.

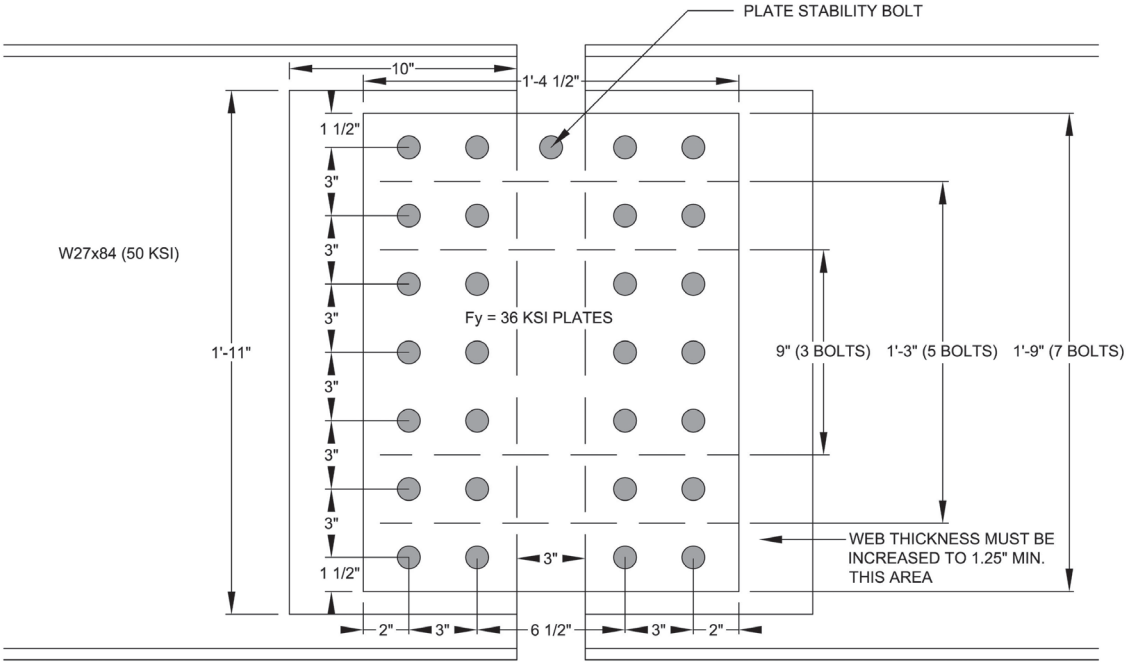

Fig. 4. Splice plate geometry.

Table 1. Measured Splice Plate Material Properties			
Heat	**F_y (ksi)**	**F_u (ksi)**	**Elongation**
1	49.5	72.1	N/A
2	48.4	63.7	47%
3	71.8	88.1	N/A

Table 2. Specimen Matrix

	Test No.	Bolt Rows (A90 Bolts)	Bolt Diameter (in.)	Measured Plate Thickness (in.)	Height (in.)	Width (in.)	Tightening Method
Heat 1	3-3/4-H1-3/8-A	3	¾	0.370	9	16.5	Impact Wrench
	3-3/4-H1-3/8-B	3	¾	0.370	9	16.5	Spud Wrench
	5-3/4-H1-3/8-A	5	¾	0.370	15	16.5	Impact Wrench
	5-3/4-H1-3/8-B	5	¾	0.370	15	16.5	Impact Wrench
	7-3/4-H1-3/8-A	7	¾	0.370	21	16.5	Impact Wrench
	7-3/4-H1-3/8-B	7	¾	0.370	21	16.5	Impact Wrench
Heat 2	3-1-H2-5/8-A	3	1	0.620	9	16.5	Impact Wrench
	3-1-H2-5/8-B	3	1	0.620	9	16.5	Impact Wrench
	3-1-H2-5/8-C	3	1	0.620	9	16.5	Impact Wrench
	5-1-H2-5/8-A	5	1	0.620	15	16.5	Impact Wrench
	5-1-H2-5/8-B	5	1	0.620	15	16.5	Impact Wrench
	5-1-H2-5/8-C	5	1	0.620	15	16.5	Impact Wrench
Heat 3	5-1-H3-3/8-A	5	1	0.381	15	16.5	Spud Wrench
	5-1-H3-3/8-B	5	1	0.381	15	16.5	Impact Wrench

Steel from three heats was used for the specimens. The first heat was a sheet of A36 steel, ⅜ in. × 18 in. × 20 ft. The second heat was also A36 steel, ⅝ in. × 18 in. × 20 ft. These are referred to as Heats 1 and 2, respectively. All plates fabricated from this material were cut with a standard steel bandsaw and all holes were punched using laboratory equipment. The plates from the third heat consisted of ⅜-in. fabricated plates with 13⁄16-in. punched holes and were provided by the sponsor. It was found through tensile testing that these plates had a very high strength, and therefore, bolt shear would be the governing limit state if ¾-in.-diameter bolts were used. Therefore, 1 1⁄16-in.-diameter holes were drilled to accommodate 1-in. A490 bolts, eliminating bolt shear as the controlling limit state. This material is referred to as Heat 3. Table 1 is a summary of tensile coupon test results for the steel from the three heats.

Connection geometry, measured splice plate thickness, and method of tightening are shown in Table 2. The tests are organized by heat number, then by number of bolts and are designated by number of bolts, bolt size, heat number, and nominal plate thickness. For instance, Test 3-3/4-H1-3/8-A has three bolt rows, ¾-in.-diameter bolts, and steel from Heat 1 of ⅜-in. thickness. The A at the end signifies that this is the first test of this type.

Test Results

Table 3 is a summary of the test results. The failure mode for all tests was either flexural rupture of the splice plate or when the mid-span beam deflection reached the limit of the test setup, approximately 8 in. The tests with ⅜-in. plates from Heat 1 all failed by flexural rupture. The tests with ⅝-in. plate from Heat 2 were stopped due to excessive deflection prior to flexure rupture, except for Tests 5-1-H2-5/8-A and 5-1-H2-5/8-C, which failed by flexural rupture. Tests 5-1-H3-3/8-A and 5-1-H3-3/8-B were conducted with higher yield stress material, Heat 3. Test 5-1-H3-3/8-A was stopped due to excessive deflection, and Test 5-1-H3-3/8-B

Table 3. Test Results					
	Test No.	No. of Bolt Rows	Observed First Yield Moment M_{ye} (kip-ft)	Maximum Applied Moment M_{ue} (kip-ft)	Failure Mode
Heat 1	3-3/4-H1-3/8-A	3	23	34.2	Flexural Rupture
	3-3/4-H1-3/8-B	3	22	31.5	Flexural Rupture
	5-3/4-H1-3/8-A	5	67	91.7	Flexural Rupture
	5-3/4-H1-3/8-B	5	70	88.8	Flexural Rupture
	7-3/4-H1-3/8-A	7	118	167.1	Flexural Rupture
	7-3/4-H1-3/8-B	7	122	175.4	Flexural Rupture
Heat 2	3-1-H2-5/8-A	3	39	48.3	Excessive Deflection
	3-1-H2-5/8-B	3	37	53.6	Excessive Deflection
	3-1-H2-5/8-C	3	35	51.5	Excessive Deflection
	5-1-H2-5/8-A	5	106	169.5	Flexural Rupture
	5-1-H2-5/8-B	5	107	134.4	Excessive Deflection
	5-1-H2-5/8-C	5	100	152.1	Flexural Rupture
Heat 3	5-1-H3-3/8-A	5	70	107.3	Excessive Deflection
	5-1-H3-3/8-B	5	84	117.8	Flexural Rupture

Table 4. Comparison of Test Data with Predicted First Yield Moment Values						
	Test No.	First Yield Moment M_{ye} (kip-ft)	F_y (ksi)	S_{gross} (in.^{3})	F_yS_{gross} (kip-ft)	$\frac{F_yS_{gross}}{M_{ye}}$
Heat 1	3-3/4-H1-3/8-A	23	49.5	5.00	20.6	0.89
	3-3/4-H1-3/8-B	22	49.5	5.00	20.6	0.93
	5-3/4-H1-3/8-A	67	49.5	13.88	57.3	0.85
	5-3/4-H1-3/8-B	70	49.5	13.88	57.3	0.82
	7-3/4-H1-3/8-A	118	49.5	27.20	112	0.95
	7-3/4-H1-3/8-B	122	49.5	27.20	112	0.92
Heat 2	3-1-H2-5/8-A	39	48.4	8.37	33.8	0.86
	3-1-H2-5/8-B	37	48.4	8.37	33.8	0.91
	3-1-H2-5/8-C	35	48.4	8.37	33.8	0.96
	5-1-H2-5/8-A	106	48.4	23.25	93.8	0.88
	5-1-H2-5/8-B	107	48.4	23.25	93.8	0.88
	5-1-H2-5/8-C	100	48.4	23.25	93.8	0.93
Heat 3	5-1-H3-3/8-A	70	71.8	14.29	85.5	1.22
	5-1-H3-3/8-B	84	71.8	14.29	85.5	1.02

failed by flexural rupture. Photographs of tested plates are shown in Figure 5.

Two representative moment at the bolt line vs. vertical deflection plots are shown in Figure 6. Test 3-3/4-H1-3/8-A failed by flexural rupture and Test 3-1-H2-5/8-A was stopped because of excessive deflection. The nonlinear response up to approximately 10 kip-ft is attributed to movement at the bolt holes since the bolts were only snug tight. The experimental yield point is defined as the intersection of the elastic and strain hardening slopes of the curves, as shown in Figure 6. Also shown in the figure are the predicted plate yield moments for each test, F_yS_{gross}, using measured material properties.

Table 4 compares the experimental first yield moments, M_{ye}, to the predicted first yield moments determined using measured plate properties for all tests. All moments shown are per splice plate. A value of the ratio of the experimental first yield moment-to-predicted first yield moment less than 1.0 indicates that the prediction is conservative. Overall, the test results show good agreement with the predicted first yield moment, F_yS_{gross}. The results are somewhat conservative for Heats 1 and 2 (mean ratio = 0.90). For Heat 3, the experimental yield moment of Test 5-1-H3-3/8-A is 122% of the predicted first yield moment. However, the same plate material was used in Test 5-1-H3-3/8-B and the ratio is 1.02. Excluding Test 5-1-H3-3/8-A, the mean ratio for the remaining 13 tests is 0.91 or approximately 9% conservative.

COMPARISON OF EXPERIMENTAL MOMENT WITH CURRENT DESIGN MODELS

Comparisons of predicted moments, F_uS_{net}, F_yZ_{gross}, and F_uZ_{net}, from current design models with the maximum applied experimental moment, M_{ue}, are shown in Table 5. All moments are per plate, and all predicated moments were determined using measured material properties.

The net elastic section modulus, S_{net}, was determined from:

$$S_{net} = \frac{t}{6}\left[d^2 - \frac{s^2 n\left(n^2-1\right)\left(d_h'\right)}{d}\right] \quad (5)$$

where

d = depth of the plate
s = bolt spacing
n = number of bolts in one vertical row
d_h' = effective diameter of the bolt hole

The vertical edge distances are assumed to be $s/2$, and the vertical dimension of the plate is then $d = ns$. Because standard size holes were used, d_h' was taken as the bolt diameter plus ⅛ in. The gross plastic section modulus, Z_{gross}, was calculated using:

$$Z_{gross} = \frac{td^2}{4} \quad (6)$$

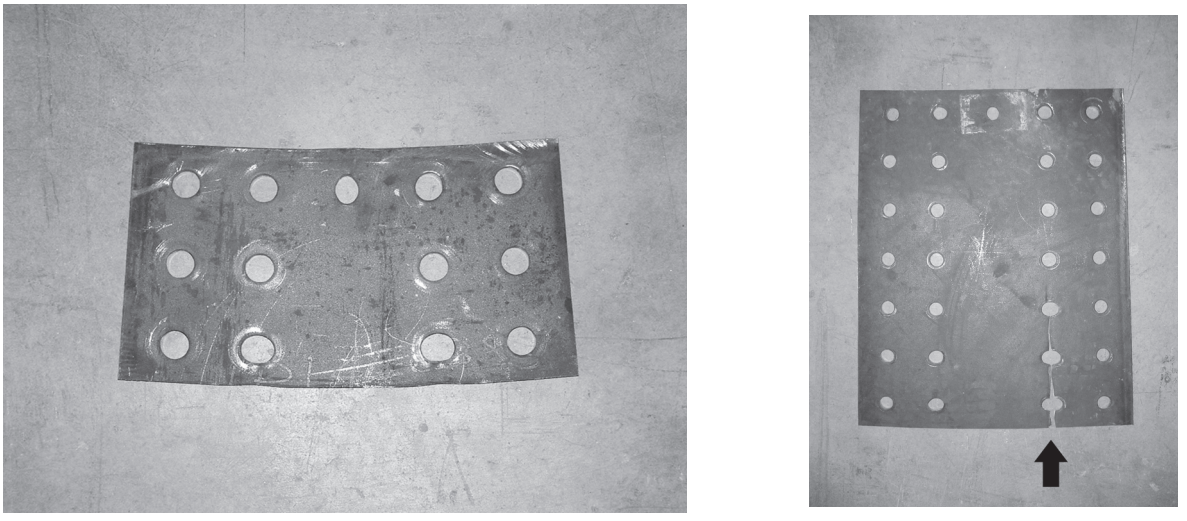

(a) (b)

Fig. 5. Photographs of tested plates.

The net plastic section modulus, Z_{net}, for an odd number of bolt rows is

$$Z_{net} = \frac{1}{4}t\left(s - d_h'\right)\left(n^2 s + d_h'\right) \tag{7}$$

and, for an even number of bolt rows

$$Z_{net} = \frac{1}{4}t\left(s - d_h'\right)n^2 s \tag{8}$$

For both equations, the vertical edge distances are assumed to be $s/2$ with a plate depth of ns.

Also shown in Table 5 are the ratios of the predicted moments ($F_u S_{net}$, $F_y Z_{gross}$, and $F_u Z_{net}$) to the maximum experimental moments using measured plate properties. The predicted strength using $F_u S_{net}$ gives very conservative results with significant scatter.

For Heat 1, the predicted strengths, $F_y Z_{gross}$ and $F_u Z_{net}$, are within 5% of each other. The minimum predicted strength for all six Heat 1 tests is $F_y Z_{gross}$; however, the experimental failure mode for all tests was flexural rupture. The mean value of the minimum predicted strength-to-maximum experimental moment ratios, $F_y Z_{gross}/M_{ue}$, is 0.96, or approximately 4% conservative.

For Heat 2, the predicted limit state strengths are flexural rupture for all six tests. Four of the six tests were terminated before flexural rupture because of excessive deflection; continued loading may have caused rupture. The mean value of the minimum predicted strength-to-maximum experiment moment ratios, $F_u Z_{net}/M_{ue}$, is 0.83, or approximately 17% conservative.

The predicted strengths for the two Heat 3 tests are flexural rupture. One test was terminated because of excessive deflection and the other failed by flexural rupture. The mean value of the minimum predicted strength-to-maximum experimental moment ratios, $F_u Z_{net}/M_{ue}$, is 0.89, or approximately 11% conservative.

The mean value of the predicted controlling limit state moment to the maximum experimental moment ratios for all 14 tests is 0.89 with no value exceeding 1.0, but with some scatter.

ALTERNATIVE NEW DESIGN MODEL

An alternative design model for flexural rupture is to assume that bolt holes in the compression region of the plate can be neglected when computing the net plastic section modulus (as is done, for instance, in columns), resulting in a modified section modulus, Z'_{net}. Thus,

$$M_n = F_u Z'_{net} \tag{9}$$

with

$$Z'_{net} = \sum |A_i d_i| \tag{10}$$

where

A_i = area of plate section i

d_i = distance from the center of section i to the plastic neutral axis, as explained in Figure 7

The plastic neutral axis is located by setting the area of the plate in compression equal to the area of the plate in tension.

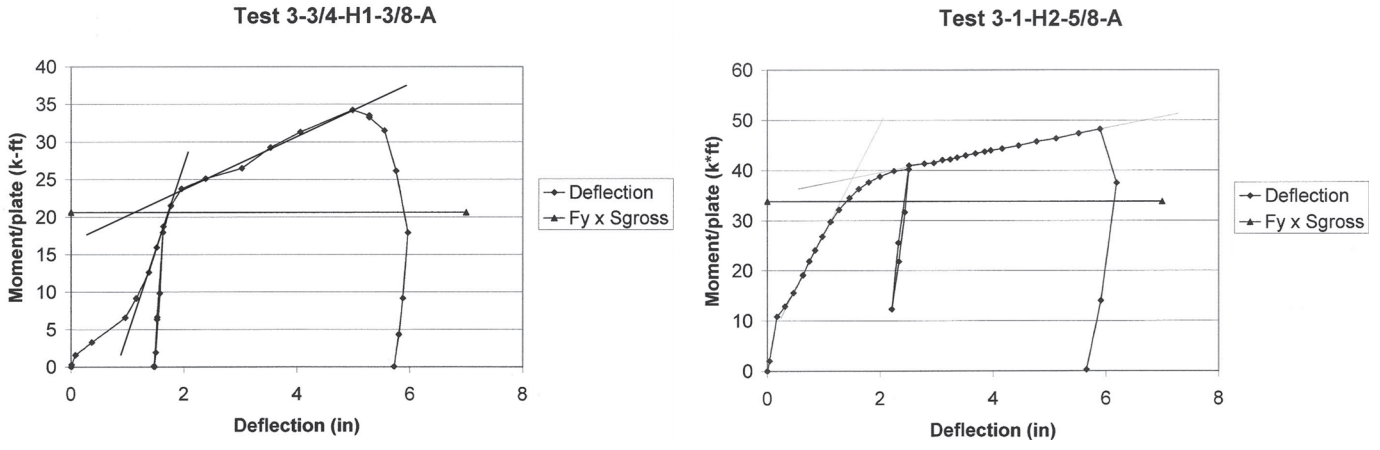

(a) (b)

Fig. 6. Representative moment vs. deflection plots.

Table 5. Comparison of Test Data with Existing Design Models												
	Test No.	M_{ue} (kip-ft)	F_y (ksi)	F_u (ksi)	S_{net} (in.^{3})	Z_{gross} (in.^{3})	Z_{net} (in.^{3})	Z'_{net} (in.^{3})	$\frac{F_uS_{net}}{M_{ue}}$	$\frac{F_yZ_{gross}}{M_{ue}}$	$\frac{F_uZ_{net}}{M_{ue}}$	$\frac{F_uZ'_{net}}{M_{ue}}$
Heat 1	3-3/4-H1-3/8-A	34.2	49.5	72.1	3.70	7.49	5.48	6.24	0.65	0.90	0.96	1.10
	3-3/4-H1-3/8-B	31.5	49.5	72.1	3.70	7.49	5.48	6.24	0.70	0.98	1.04	1.19
	5-3/4-H1-3/8-A	91.7	49.5	72.1	9.97	20.81	14.91	17.26	0.65	0.94	0.98	1.13
	5-3/4-H1-3/8-B	88.8	49.5	72.1	9.97	20.81	14.91	17.26	0.67	0.97	1.01	1.17
	7-3/4-H1-3/8-A	167.1	49.5	72.1	19.42	40.79	29.07	33.83	0.70	1.00	1.05	1.21
	7-3/4-H1-3/8-B	175.4	49.5	72.1	19.42	40.79	29.07	33.83	0.66	0.96	1.00	1.16
Heat 2	3-1-H2-5/8-A	48.3[1]	48.4	63.7	5.58	12.56	8.17	9.68	0.61	1.05	0.90	1.06
	3-1-H2-5/8-B	53.6[1]	48.4	63.7	5.58	12.56	8.17	9.68	0.55	0.95	0.89	0.96
	3-1-H2-5/8-C	51.5[1]	48.4	63.7	5.58	12.56	8.17	9.68	0.57	0.98	0.84	1.00
	5-1-H2-5/8-A	169.5	48.4	63.7	14.88	34.88	22.12	26.83	0.47	0.83	0.69	0.84
	5-1-H2-5/8-B	134.4[1]	48.4	63.7	14.88	34.88	22.12	26.83	0.59	1.05	0.87	1.06
	5-1-H2-5/8-C	152.1	48.4	63.7	14.88	34.88	22.12	26.83	0.52	0.93	0.77	0.94
Heat 3	5-1-H3-3/8-A	107.3[1]	71.8	88.1	9.14	21.43	13.60	16.49	0.63	1.19	0.93	1.13
	5-1-H3-3/8-B	117.8	71.8	88.1	9.14	21.43	13.60	16.49	0.57	1.09	0.85	1.03

[1]Test terminated due to excessive deflection.

The ratio of the predicted moment from Equation 9 using measured material properties to the maximum experimental moment for each test is given in Table 5. The ratios are larger (less conservative) than those using F_uZ_{net} for all 14 tests. For Heats 2 and 3, the ratios using the moment from Equation 9 are very near the ratios M_{ue}/F_yZ_{gross}. The mean ratio for the predicted controlling limit state (smaller of F_yZ_{gross} and $F_uZ'_{net}$) for the 14 tests is 0.98, with some values greater than 1.0.

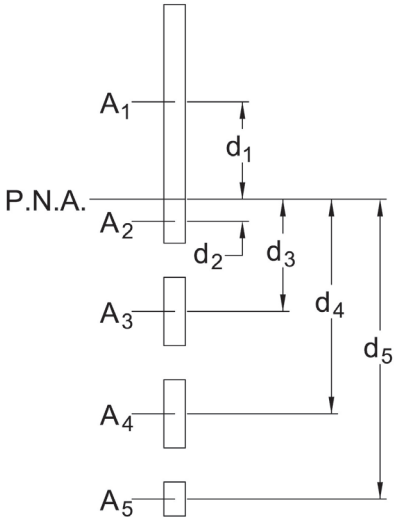

Fig. 7. Terms used in calculation of Z'_{net}.

OVERALL EVALUATION

From the results of the 14 tests, the minimum of the predicted moments F_yZ_{gross} and F_uZ_{net}, or F_yZ_{gross} and $F_uZ'_{net}$, matches the controlling experimental failure mode and generally provides an accurate prediction of the maximum experimental moment. However, the use of $F_uZ'_{net}$ resulted in unconservative predictions for all of the Heat 1 tests.

It is important to note that the maximum experimental moments were obtained only after very large deflections and that restraints were used to prevent compression flange movement at the connections as well as splice plate buckling as explained earlier.

A significant contribution to the deflection was movement of the bolts prior to application of load. When the erection supports were removed, the test setup frequently showed large initial deflections due to self-weight. This was especially evident in the plates with three rows of bolts and was caused by movement of the bolts within the standard-size holes. Initial stiffness was affected by the method used to tighten the bolts; impact wrench tightening resulted in a slightly stiffer connection. However, the maximum moment strengths were not affected.

Despite the precautions taken to prevent buckling, some local buckling was observed in the compression region of several plates. It is emphasized that to achieve the experimental moment strength in this study, it was necessary to use an additional bolt through the center of the plate in line with the top row of bolts as shown in Figure 4.

Table 6. Comparison of Available Moment Strengths F_yZ_{gross} and F_uZ_{net}					
No. of Bolts	Bolt Diameter (in.)	Nominal Moment Strength			
		F_y = 36 ksi	F_u = 58 ksi	F_y = 50 ksi	F_u = 65 ksi
		$0.9F_yZ_{gross}$ (kip-ft)	$0.75F_uZ_{net}$ (kip-ft)	$0.9F_yZ_{gross}$ (kip-ft)	$0.75F_uZ_{net}$ (kip-ft)
2	¾	24.3	23.1	33.8	25.9
	⅞	24.3	21.8	33.8	24.4
	1	24.3	20.4	33.8	22.9
3	¾	54.7	53.7	75.9	60.2
	⅞	54.7	50.8	75.9	56.9
	1	54.7	47.8	75.9	53.6
4	¾	97.2	92.4	135	103
	⅞	97.2	87.0	135	97.5
	1	97.2	81.6	135	91.4
5	¾	151	146	210	163
	⅞	151	137	210	154
	1	151	129	210	145
6	¾	218	208	303	233
	⅞	218	195	303	219
	1	218	183	303	205
7	¾	297	284	413	319
	⅞	297	268	413	300
	1	297	251	413	282
8	¾	388	369	540	414
	⅞	388	348	540	390
	1	388	326	540	365
9	¾	492	469	683	526
	⅞	492	442	683	495
	1	492	414	683	464
10	¾	607	577	843	647
	⅞	607	543	843	609
	1	607	509	843	571

COMPARISON OF NOMINAL MOMENT STRENGTHS

Table 6 shows available LFRD moment strengths using $0.9F_yZ_{gross}$ and $0.75F_uZ_{net}$ for connections with two to 10 bolts using nominal material properties, for A36 and A572 Grade 50 steels, s = 3 in., vertical edge distance $s/2$ = 1.5 in., plate thickness of 1 in., and bolt diameters of ¾, ⅞ and 1 in. The data show that for every connection, flexural rupture, F_uZ_{net}, is the controlling limit state. It is noted that these are relative values and actual connection strength may be governed by bolt shear or another limit state.

DESIGN RECOMMENDATIONS

This study indicates that design models used prior to the publication of the 13th Edition AISC *Steel Construction Manual* (AISC, 2005b) for determining bracket plate and web splice nominal moment strength are overly conservative. From the test results, the available moment strength in LRFD, ϕM_n, can safely be calculated as the minimum of $0.9F_yZ_{gross}$ and $0.75F_uZ_{net}$, or in ASD as the minimum of $F_yZ_{gross}/1.67$ and $F_uZ_{net}/2.0$, which are the current AISC Manual design models. Consequences of large deflections and supported member or plate instability must be considered when these values

are used. If deflection is a concern, the factored loads should also be checked against $0.9F_yS_{gross}$.

Lateral stability is extremely important to reach the maximum plastic moment; therefore, these results are not recommended for coped beams or unbraced bracket plates.

ACKNOWLEDGMENTS

Funding for this study was provided by Cives Steel Company. The contributions of William A. Thornton, Larry S. Muir, and Rob Kerr are greatly appreciated.

REFERENCES

AISC (2001), *Manual of Steel Construction, Load and Resistance Factor Design,* 3rd Edition, American Institute of Steel Construction, Chicago, IL.

AISC (2005a), *Specification for Structural Steel Buildings*, American Institute of Steel Construction, Chicago, IL, March 9.

AISC (2005b), *Steel Construction Manual*, 13th Edition, American Institute of Steel Construction, Chicago, IL.

AISC (2005c), *Design Examples V.13.0*, American Institute of Steel Construction, Chicago, IL.

Thornton, W.A. and Kane, T. (1999), *Handbook of Structural Steel Connection Design and Details*, McGraw-Hill Book Company, New York.